

## Cycloaddition

International Edition: DOI: 10.1002/anie.201602384  
German Edition: DOI: 10.1002/ange.201602384

## Neutral Diboron Analogues of Archetypal Aromatic Species by Spontaneous Cycloaddition

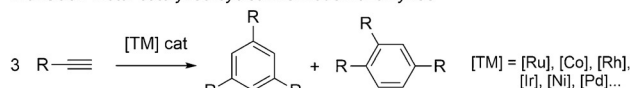
Merle Arrowsmith, Julian Böhnke, Holger Braunschweig,\* Mehmet Ali Celik, Christina Claes, William C. Ewing, Ivo Krummenacher, Katharina Lubitz, and Christoph Schneider

**Abstract:** Among the numerous routes organic chemists have developed to synthesize benzene derivatives and heteroaromatic compounds, transition-metal-catalyzed cycloaddition reactions are the most elegant. In contrast, cycloaddition reactions of heavier alkene and alkyne analogues, though limited in scope, proceed uncatalyzed. In this work we present the first spontaneous cycloaddition reactions of lighter alkene and alkyne analogues. Selective addition of unactivated alkynes to boron–boron multiple bonds under ambient conditions yielded diborocarbon equivalents of simple aromatic hydrocarbons, including the first neutral  $6\pi$ -aromatic diborabenzene compound, a  $2\pi$ -aromatic triplet biradical 1,3-diborete, and a phosphine-stabilized  $2\pi$ -homoaromatic 1,3-dihydro-1,3-diborete. DFT calculations suggest that all three compounds are aromatic and show frontier molecular orbitals matching those of the related aromatic hydrocarbons,  $C_6H_6$  and  $C_4H_4^{2+}$ , and homoaromatic  $C_4H_5^+$ .

The selective construction of Hückel-aromatic carbo- and heterocycles has mobilized countless researchers throughout the last two centuries.<sup>[1]</sup> Today aromatic compounds account for nearly one-third of all small organic molecules produced on an industrial scale<sup>[2]</sup> and are key components in such diverse areas as drug development,<sup>[3]</sup> chemical and biological molecular recognition,<sup>[4]</sup> energetic materials,<sup>[5]</sup> and fuel cells.<sup>[6]</sup> Since the discovery of nickel-catalyzed acetylene cyclotrimerization in the 1940s,<sup>[7]</sup> late transition metal catalyzed alkyne [2+2+2] cycloaddition reactions have been widely used as the most elegant synthetic route to access benzene derivatives (Figure 1).<sup>[8]</sup> Due to large enthalpic and entropic barriers, however, the vast majority of alkyne cycloaddition reactions require either a catalyst or forcing thermal conditions.<sup>[9]</sup>

In contrast, alkene and alkyne analogues of the heavier p-block elements tend to undergo facile uncatalyzed cycloaddition reactions with unactivated alkynes. Disilenes, digermenes, and distannenes, for example, undergo formal [2+2] cycloaddition with polar alkynes to form the corresponding

Transition metal catalyzed cyclotrimerization of alkynes



Uncatalyzed alkyne cycloaddition to heavier homodinuclear p-block multiple bonds

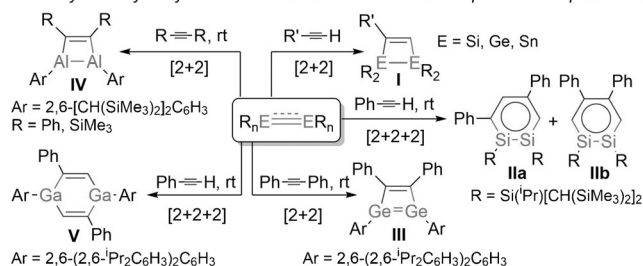


**Figure 1.** Alkyne cycloaddition to multiply bonded, homodinuclear p-block species.

1,2-ditetrel-3-cyclobutenes **I** (Figure 1).<sup>[10]</sup> For some bridged distannenes, this reaction was shown to be reversible.<sup>[11]</sup> Recently the isolation of the first heavier Group 14 alkyne analogues has also enabled the synthesis of the first  $6\pi$ -aromatic 1,2-disilabenzene derivatives, **IIa** and **IIb**, and  $4\pi$ -antiaromatic 1,2-digermacyclobutadiene **III** by alkyne cycloaddition (Figure 1).<sup>[12]</sup> With regards to heavier Group 13 alkene analogues, Tokitoh and co-workers described the addition of alkynes to a dialumene–benzene adduct leading to the formation of 1,2-dialuminacyclobut-3-enes (**IV**) (Figure 1),<sup>[13]</sup> while Power and co-workers synthesized 1,4-digallacyclohexa-2,5-diene **V** by double cycloaddition of phenylacetylene to a digallene (Figure 1).<sup>[14]</sup>

Owing to the increasing popularity of boron-containing aromatics as therapeutic agents<sup>[15]</sup> and luminescent hybrid organic molecules,<sup>[16]</sup> controlled and efficient cycloaddition routes towards these compounds would be highly desirable. Thus far, however, even the synthesis of such a simple molecule as the benzene analogue 1,2-dihydro-1,2-azaborabenzene [ $BNC_4H_6$ ] necessitates a complex seven-step route,<sup>[17]</sup> whereas the neutral borabenzene molecule [ $BC_5H_5$ ] has thus far eluded synthesis. Requisite for controlled cycloaddition, stable, neutral compounds containing B–B multiple bonds remained unknown until the report in 2007 by Robinson and co-workers of the first N-heterocyclic carbene (NHC)-stabilized diborene.<sup>[18]</sup> Since then, our group has synthesized the first compound with a B–B triple bond as well as a cyclic (alkyl)(amino)carbene (CAAC)-stabilized diboracumulene.<sup>[19]</sup>

Herein we now report the selective synthesis of a variety of novel  $2\pi$ - and  $6\pi$ -aromatic borocarbon heterocycles by

[\*] Dr. M. Arrowsmith, J. Böhnke, Prof. Dr. H. Braunschweig, Dr. M. A. Celik, Dr. C. Claes, Dr. W. C. Ewing, Dr. I. Krummenacher, K. Lubitz, Dr. C. Schneider  
Institut für Anorganische Chemie  
Julius-Maximilians-Universität Würzburg  
Am Hubland, 97074 Würzburg (Germany)  
E-mail: h.braunschweig@uni-wuerzburg.de  
Homepage: <http://www.braunschweiggroup.de/>

Supporting information for this article (general experimental details, characterization data for all reported compounds, and details of the DFT calculations) can be found under:  
<http://dx.doi.org/10.1002/anie.201602384>.

spontaneous cycloaddition of unactivated alkynes with diborenes and diboracumulenes, making these the first uncatalyzed cycloaddition reactions of lighter alkene and alkyne analogues.

In preliminary experiments NHC-stabilized diborenes displayed no reactivity towards acetylenes even under forcing or photolytic conditions. Therefore the phosphine-stabilized diborene **VI**<sup>[20]</sup> was employed in the hope that the lability of the  $\text{PMe}_3$  ligands would enable cycloaddition. Under photolytic conditions in  $\text{Et}_2\text{O}$ , the phosphine-stabilized diborene **VI** underwent quantitative reaction within 4 hours at room temperature with one equivalent of 2-butyne to yield a colorless solution (Figure 2). Removal of the solvent and washing

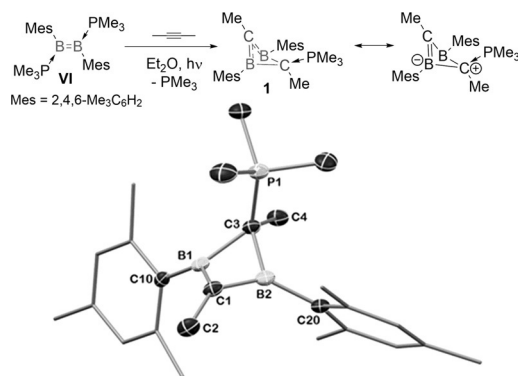


**Figure 2.** Reaction of 2-butyne with diborene **VI**. X-ray crystallographic structure of one of the molecules of **1** present in the asymmetric unit.<sup>[31]</sup> Thermal ellipsoids are depicted at the 50% probability level. For clarity, hydrogen atoms and thermal ellipsoids of the mesityl carbon atoms are removed. Selected bond lengths [Å] and angles [°]: B1–C1 1.486(4), B2–C1 1.465(4), B1–C3 1.630(4), B2–C3 1.666(4), B1...B2 1.878(4), C3–P1 1.759(2); B1–C1–B2 79.0(2), B1–C3–B2 69.5(2), C1–B1–C3 99.7(2), C1–B2–C3 98.9(2).

of the residue with pentane yielded a colorless solid presenting a broad  $^{11}\text{B}$  NMR singlet at 25.6 ppm, characteristic of a three-coordinate boron center, and a new broad  $^{31}\text{P}$  NMR resonance at 23.1 ppm, both significantly downfield of the diborene NMR resonances at  $\delta_{11\text{B}}$  16.7 and  $\delta_{31\text{P}}$  –24.4 ppm, respectively.<sup>[20]</sup>

Single-crystal X-ray analysis revealed an asymmetric unit comprising two molecules of compound **1**, a monophosphine-stabilized homoaromatic 1,3-dihydro-1,3-diborete in which a phosphine ligand has shifted from boron to one of the carbon atoms of the central BCBC ring (Figure 2). The latter presents a butterfly structure with carbon atoms located at the tips of the wings and a puckering angle of ca. 34.5°. Whereas the analogous reaction with a dialumene precursor yields the 1,2-dihydro-1,2-dialumete **IV** (Figure 1),<sup>[13]</sup> the 1,3-isomer is obtained in this case. Although this reaction involves formal cleavage of  $\text{C}\equiv\text{C}$  and  $\text{B}=\text{B}$  bonds, previous synthetic and theoretical studies have shown that 1,2-dihydro-1,2-diboretes spontaneously rearrange to the thermodynamically more stable 1,3-isomer.<sup>[21]</sup> It is thus likely that diborene **VI** first undergoes the expected [2+2] cycloaddition to form the kinetic 1,2-dihydro-1,2-diborete, which immediately rearranges to the thermodynamic product, **1**. The short B–C

bond lengths to the  $\text{sp}^2$ -hybridized C1 atom [1.486(4), 1.465(4) Å] are indicative of a  $2\pi$ -homoaromatic system delocalized over B1C1B2, whereas the B–C bonds to the  $\text{sp}^3$ -hybridized C3 atom [1.630(4), 1.666(4) Å] are within the upper range of B–C single bonds. Compound **1** is thus structurally similar to the allenyl-bridged 1,3-dihydro-1,3-diborete reported by Berndt and co-workers.<sup>[22]</sup> The P1–C3 distance [1.759(2) Å] is typical for a P→C donor–acceptor bond; the  $\text{PMe}_3$  donor moiety thus stabilizes the build-up of positive charge on C3 (mesoionic resonance structure in Figure 2).

Due to the enhanced  $\pi$ -acceptor properties of CAAC versus NHC ligands, the CAAC-stabilized diboracumulene **VII** may be regarded as an intermediate bonding case between electron-precise diborenes ( $\text{B}=\text{B}$ ) and diborynes ( $\text{B}\equiv\text{B}$ ).<sup>[19]</sup> It was thus of interest to compare the reactivity of **VII** towards alkynes with that of **VI**. A violet solution of **VII** in benzene, left unstirred under an atmosphere of propyne, turned deep blue over the course of one day at room temperature (Figure 3). NMR spectroscopic analysis of the

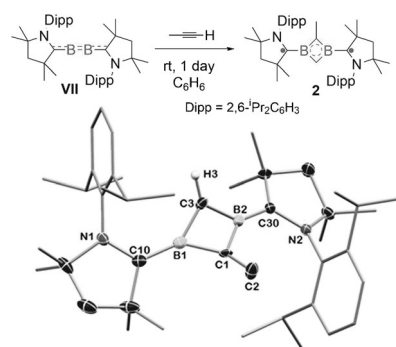


**Figure 3.** Synthesis of the triplet biradical 1,3-diborete **2** from the addition of propyne to **VII**. X-ray crystallographic structure of **2**.<sup>[31]</sup> Thermal ellipsoids are depicted at the 50% probability level. For clarity, hydrogen atoms and thermal ellipsoids of the mesityl carbon atoms are removed. Selected bond lengths [Å] and angles [°]: B1–C1 1.511(9), B2–C1 1.60(1), B1–C3 1.48(1), B2–C3 1.57(1), C1...C3 1.81(2), B1–C10 1.498(3), B2–C30 1.499(3); B1–C1–B2 96.4(6), B1–C3–B2 99.2(6), C1–B1–C3 74.4(6), C1–B2–C3 69.6(5).

reaction mixture showed no  $^{11}\text{B}$  NMR resonance and only very broad and weak  $^1\text{H}$  NMR signals, suggesting the formation of a paramagnetic species. This was further confirmed by an EPR measurement of a frozen-solution sample of **2** in 2-methyltetrahydrofuran which yielded a weak half-field signal and a four-line spectrum in the  $g=2$  region attributable to the triplet state of biradical **2** (Figure S3).

Slow evaporation of the solvent from the deep-blue reaction mixture yielded blue crystals suitable for X-ray crystallography. This revealed the structure of compound **2**, comprising a central four-membered BCBC ring, supported by two boron-coordinated CAAC ligands (Figure 3). As in compound **1** the core ring adopts a butterfly structure, this time with boron atoms located at the tips of the wings, a puckering angle of 40.2°, and two  $\text{sp}^2$ -hybridized endocyclic carbon atoms. Bond lengths and angles within the BCBC ring are reminiscent of those in the known 1,3-dihydro-1,3-

diborete species  $[(^i\text{Pr}_2\text{N})\text{BCH}]_2$ , suggesting a similar  $2\pi$ -aromatic electronic configuration.<sup>[23]</sup> As a result, the two unpaired electrons must be localized on the CAAC ligands and not within the 1,3-diborete ring. The B–C<sub>CAAC</sub> bond lengths [1.498(2), 1.500(2) Å] are significantly longer than in the boracumulene **VII** [1.459(2), 1.458(2) Å],<sup>[19]</sup> but still short for covalent single or pure  $\sigma$ -donor bonds, suggesting some degree of  $\pi$ -backbonding from the cyclic system to the CAAC carbon atom. The preferential formation of a biradical [CAAC]-stabilized  $2\pi$ -aromatic diborete instead of a neutral CAAC-stabilized  $4\pi$ -antiaromatic 1,3-diboracyclobutadiene may be explained by the higher stability of the aromatic system combined with the well-known ability of CAAC ligands to delocalize electron density and form [CAAC] radicals.<sup>[24]</sup> Furthermore, while a butterfly conformation may seem counterintuitive for an aromatic ring, *ab initio* molecular orbital theory studies have shown that the puckered structure of  $2\pi$ -aromatic 1,3-diboretes is significantly more stable than the planar conformation.<sup>[25]</sup> Unlike diborene **VI**, **VII** did not display any reactivity towards 2-butyne under these reaction conditions.

Although the analogous reaction with acetylene (Figure 4) also yielded a deep-blue solution, the resulting product, **3**, proved to be diamagnetic and presented a single  $^{11}\text{B}$  NMR resonance at 24.8 ppm (Figure 4). Examination of the  $^1\text{H}$  NMR spectrum also provided a characteristic singlet at 7.31 ppm, integrating at 4H relative to the CAAC-derived resonances, and correlating with a  $^{13}\text{C}$  resonance at 150.5 ppm, hinting at the formation of a six-membered  $6\pi$ -aromatic  $\text{B}_2\text{C}_4$  ring. This was later confirmed by X-ray diffraction analysis of **3**, which revealed the expected 1,4-diborabenzene ring supported by two boron-coordinated CAAC ligands (Figure 4). *Ab initio* calculations have shown the 1,4-diborabenzene isomer to be significantly more stable than the other possible product of this reaction, the 1,2-isomer.<sup>[26]</sup> While dianionic aromatic diboratabenzenes have been known since the 1980s,<sup>[27]</sup> compound **3** is, to our

knowledge, the first example of an isolated, neutral  $6\pi$ -aromatic diborabenzene species.

Unlike the  $\text{B}_2\text{C}_2$  ring of **2**, the  $\text{B}_2\text{C}_4$  ring of compound **3** is perfectly planar, with angles close to the idealized  $120^\circ$  of a benzene ring [ $114.8(2)$ – $122.8(2)^\circ$ ]. The mean planes of both CAAC ligand frameworks are quasi-coplanar with the 1,4-diborabenzene ring (dihedral angles ca.  $7.0$  and  $7.9^\circ$ ). The B–C bonds within the ring [1.522(3)–1.540(3) Å] are elongated compared to related Lewis base stabilized aromatic borabenzene compounds [ca. 1.49 Å].<sup>[28]</sup> The C–C distances within the ring [1.372(3), 1.378(3) Å], although slightly shorter than in the related borabenzene adducts [ca. 1.40 Å],<sup>[28]</sup> are still significantly longer than the formal C–C double bonds in the related 1,4-difluoro-2,3,5,6-tetramethyl-1,4-dibora-2,5-cyclohexadiene  $\text{B}_2\text{C}_4$  ring [1.329(7) Å],<sup>[29]</sup> suggesting significant electron delocalization throughout the 1,4-diborabenzene ring. For comparison the B–C and C–C distances of the parent 1,4-diborabenzene,  $[\text{B}_2\text{C}_4\text{H}_4]$ , were calculated to be 1.452 and 1.450 Å, respectively.<sup>[26]</sup> The bond length variations within the  $\text{B}_2\text{C}_4$  ring in **3** likely arise from the  $\pi$ -acceptor properties of the supporting CAAC ligands. The elongated B–C<sub>CAAC</sub> distances [1.554(3), 1.563(3) Å], however, suggest that  $\pi$ -backbonding from the diborabenzene ring to the CAAC ligands is significantly weaker than in **VII** [B–C<sub>CAAC</sub> 1.459(2), 1.458(2) Å].<sup>[19]</sup> The formation of the six-membered diborabenzene compound **3**, when acetylene is used rather than propyne, suggests a stepwise formation mechanism via a four-membered 1,2-diborete. The fact that the reaction with excess propyne does not proceed through to the diborabenzene product under these reaction conditions may be ascribed to the larger steric demands of propyne versus acetylene hindering a second insertion. Cyclic voltammetry of compound **3** in THF showed two reversible reduction waves (vs.  $\text{Fc}/\text{Fc}^+$ ) at  $-0.81$  and  $-2.48$  V, respectively (Figure S2), hinting at the possibility of selective chemical reduction of this species.

In order to analyze the  $\pi$ -bonding in compounds **1–3**, density functional theory calculations were performed on all three structures optimized at the BP86/def2-SVP level, with **1** and **3** as singlet closed-shell and **2** as triplet biradical compounds. Structural parameters of the optimized structures were in good agreement with X-ray crystallographic data (Figure 5, Figures S6, S8, and S10). The HOMO of **1** corresponds to the delocalized  $2\pi$ -homoaromatic system of the 1,3-dihydro-1,3-diborete ring and closely resembles that of the related  $2\pi$ -homoaromatic  $\text{C}_4\text{H}_5^+$  cation (Figure 5a). The two SOMOs of **2** clearly show the two unpaired electrons to be mainly localized on the CAAC carbene carbon and nitrogen atoms, which is also confirmed by the calculated Mulliken spin densities (C: 0.57, N: 0.21) (Figure 5b). For **2** the  $2\pi$ -aromatic system of the  $\text{B}_2\text{C}_2$  ring is represented by the HOMO-4a, analogous to the HOMO of  $2\pi$ -aromatic  $\text{C}_4\text{H}_4^{2+}$  (Figure 5b). HOMO-8a also evidences  $\pi$ -backbonding from the 1,3-diborete ring to the CAAC ligands (Figure 5b). Frontier molecular orbital plots of **3** also display great similarity to those of benzene (Figure 5c) and the parent 1,4-diborabenzene.<sup>[26]</sup>

To assess the aromaticity of the borocarbon ring structures in compounds **1–3** nucleus-independent chemical shift

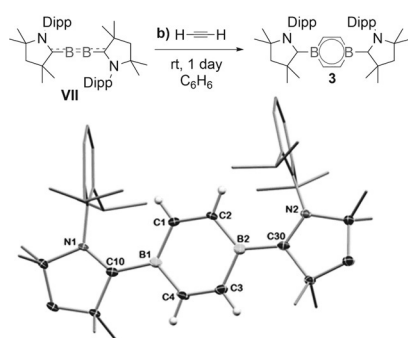


**Figure 4.** Synthesis of neutral 1,4-diborabenzene **3** from the addition of acetylene to **VII**. X-ray crystallographic structure of **3**.<sup>[31]</sup> Thermal ellipsoids are depicted at the 50% probability level. For clarity, hydrogen atoms and thermal ellipsoids of the mesityl carbon atoms are removed. Selected bond lengths [Å] and angles [ $^\circ$ ]: B1–C1 1.540(3), B1–C4 1.522(3), B2–C2 1.534(3), B2–C3 1.532(4), C1–C2 1.378(3), C3–C4 1.372(3), B1–C10 1.563(3), B2–C30 1.554(3); B1–C1–C2 122.1(2), C1–C2–B2 122.6(2), C2–B2–C3 114.7(2), B2–C3–C4 122.7(2), C3–C4–B1 122.8(2), C4–B1–C1 115.1(2).

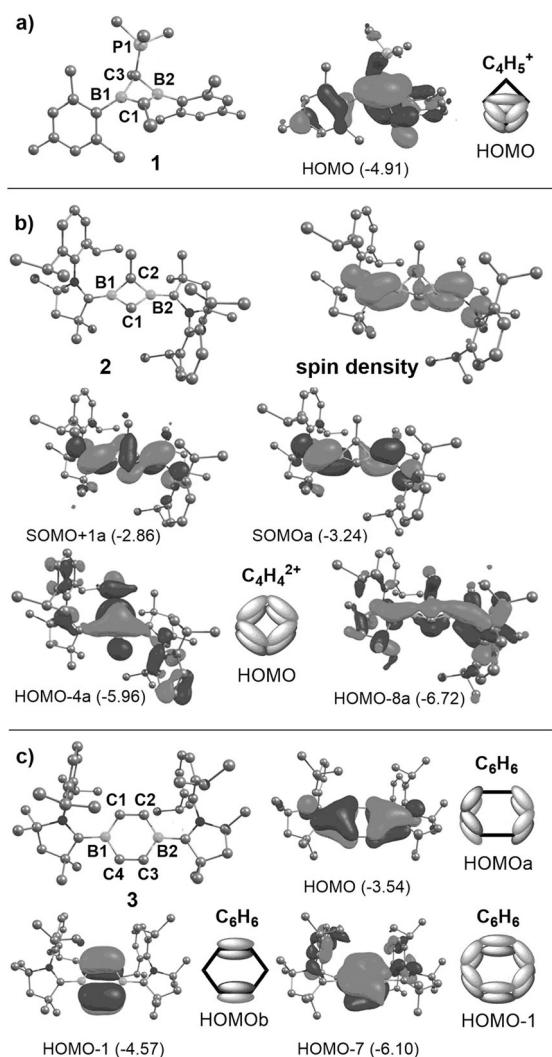


**Figure 5.** Optimized structures and frontier molecular orbitals (eV) of **1–3** at the BP86/def2-SVP level, together with schematic representations of the frontier MOs of the analogous aromatic and homoaromatic hydrocarbons. Calculated bond lengths [Å]: **1**: B1–C1 1.503, B2–C1 1.492, B1–C3 1.644, B2–C3 1.673, C3–P1 1.783. **2**: B1–C1 1.538, B2–C1 1.530, B1–C2 1.538, B2–C2 1.544. **3**: B1–C1/3 1.546, B1–C2/4 1.548, C1–C2 1.396, C3–C4 1.394.

(NICS) calculations were carried out on the structures optimized at the B3LYP/def2-TZVPP//def2-SVP level. NICS(0) values for all three compounds were found to be negative (**1** –20.62; **2** –26.35; **3** –2.86), indicating that compounds **1–3** all possess a certain degree of aromaticity (Table S1). In order to make reliable comparisons, however, the contributions of orbitals and tensor components to NICS would be required.<sup>[30]</sup> Due to the open-shell nature of compound **2** these contributions cannot be calculated for this particular species, thus precluding any meaningful comparison of the degree of aromaticity between species **1–3** and their hydrocarbon analogues.

In summary, we have presented the first examples of uncatalyzed cycloaddition reactions involving unactivated, apolar multiply bonded homodinuclear species of the second period. These reactions provide the first selective route to

diborocarbon analogues of the  $2\pi$ -aromatic cyclopropenyl cation and cyclobutenyl dication, as well as a novel neutral  $6\pi$ -aromatic diborabenzene compound. Further experimental work and calculations are currently underway to determine the mechanism of formation of these compounds, the results of which will be reported in due course. We are continuing to explore cycloaddition reactions of boron–boron multiple bonds with other unsaturated hydrocarbons and polar multiple bonds in order to access an even wider range of valuable boron-containing heterocycles.

## Acknowledgments

We acknowledge the Alexander von Humboldt Foundation (Research Fellowship for Postdoctoral Researchers to M.A.). This project was funded by the European Research Council (ERC) under the European Union Horizon 2020 Research and Innovation Program (grant agreement no. 669054).

**Keywords:** aromaticity · biradicals · boron · cycloaddition · multiple bonds

**How to cite:** *Angew. Chem. Int. Ed.* **2016**, *55*, 11271–11275  
*Angew. Chem.* **2016**, *128*, 11441–11445

- [1] E. Hückel, *Grundzüge der Theorie ungesättigter und aromatischer Verbindungen*, Chemie, Berlin, **1940**.
- [2] H.-G. Franck, J. W. Stadelhofer, *Industrial Aromatic Chemistry: Raw Materials—Processes—Products*, Springer, Berlin Heidelberg, **1988**.
- [3] T. J. Ritchie, S. J. F. Macdonald, R. J. Young, S. D. Pickett, *Drug Discovery Today* **2011**, *16*, 164–171.
- [4] L. M. Salonen, M. Ellermann, F. Diederich, *Angew. Chem. Int. Ed.* **2011**, *50*, 4808–4842; *Angew. Chem.* **2011**, *123*, 4908–4944.
- [5] L. Türker, V. Variş, *Polycyclic Aromat. Compd.* **2009**, *29*, 228–266.
- [6] G. Maier, J. Meier-Haack, *Adv. Polym. Sci.* **2008**, *216*, 1–62.
- [7] W. Reppe, O. Schichting, K. Klager, T. Toepel, *Justus Liebigs Ann. Chem.* **1948**, *560*, 1–92.
- [8] I. A. Maretina, B. I. Ionin, *Regioselective Syntheses of Polysubstituted Benzenes Catalyzed by Transition Metal Complexes in Alkynes in Cycloadditions* (Ed.: J. C. Tebb), Wiley-VCH, Weinheim, **2014**.
- [9] M. C. Bertholet, *C. R. Hebd. Seances Acad. Sci.* **1866**, *62*, 905.
- [10] a) D. J. De Young, R. West, *Chem. Lett.* **1986**, 883–884; b) S. A. Batcheller, S. Masamune, *Tetrahedron Lett.* **1988**, *29*, 3383–3384; c) V. Y. Lee, T. Fukawa, M. Nakamoto, A. Sekiguchi, B. L. Tumanskii, M. Karni, Y. Apeloig, *J. Am. Chem. Soc.* **2006**, *128*, 11643–11651.
- [11] J. Schneider, J. Henning, J. Edrich, H. Schubert, L. Wesemann, *Inorg. Chem.* **2015**, *54*, 6020–6027.
- [12] a) R. Kinjo, M. Ichinohe, A. Sekiguchi, N. Takagi, M. Sumimoto, S. Nagase, *J. Am. Chem. Soc.* **2007**, *129*, 7766–7767; b) C. Cui, M. M. Olmstead, P. P. Power, *J. Am. Chem. Soc.* **2004**, *126*, 5062–5063.
- [13] T. Agou, T. Nagata, T. Tokitoh, *Angew. Chem. Int. Ed.* **2013**, *52*, 10818–10821; *Angew. Chem.* **2013**, *125*, 11018–11021.
- [14] Z. Zhu, X. Wang, M. M. Olmstead, P. P. Power, *Angew. Chem. Int. Ed.* **2009**, *48*, 2027–2030; *Angew. Chem.* **2009**, *121*, 2061–2064.
- [15] B. C. Das, C. Z. Ding, T. Akama, Y. K. Zhang, V. Hernandez, Y. Xia, *Future Med. Chem.* **2013**, *5*, 653–676.
- [16] L. Weber, L. Böhling, *Coord. Chem. Rev.* **2015**, *284*, 236–275.

- [17] A. J. V. Marwitz, M. H. Matus, L. N. Zakharov, D. A. Dixon, S.-Y. Liu, *Angew. Chem. Int. Ed.* **2009**, *48*, 973–977; *Angew. Chem.* **2009**, *121*, 991–995.
- [18] Y. Wang, B. Quillian, P. Wei, C. S. Wannere, Y. Xie, R. B. King, H. F. Schaefer III, P. von R. Schleyer, G. H. Robinson, *J. Am. Chem. Soc.* **2007**, *129*, 12412–12413.
- [19] a) H. Braunschweig, R. D. Dewhurst, K. Hammond, J. Mies, K. Radacki, A. Vargas, *Science* **2012**, *336*, 1420–1422; b) J. Böhnke, H. Braunschweig, W. C. Ewing, C. Hörl, T. Kramer, I. Krummenacher, J. Mies, A. Vargas, *Angew. Chem. Int. Ed.* **2014**, *53*, 9082–9085; *Angew. Chem.* **2014**, *126*, 9228–9231.
- [20] P. Bissinger, H. Braunschweig, M. A. Celik, C. Claes, R. D. Dewhurst, S. Endres, H. Kelch, T. Kramer, I. Krummenacher, C. Schneider, *Chem. Commun.* **2015**, *51*, 15917–15920.
- [21] M. L. McKee, *Inorg. Chem.* **2000**, *39*, 4206–4210.
- [22] M. Menzel, H. J. Winkler, T. Ablelom, D. Steiner, S. Fau, G. Frenking, W. Massa, A. Berndt, *Angew. Chem. Int. Ed. Engl.* **1995**, *34*, 1340–1343; *Angew. Chem.* **1995**, *107*, 1476–1479.
- [23] H. Irngartinger, J. Hauck, W. Siebert, M. Hildenbrand, *Z. Naturforsch. B* **1991**, *46*, 1621–1624.
- [24] M. Soleilhavoup, G. Bertrand, *Acc. Chem. Res.* **2015**, *48*, 256–266.
- [25] P. H. M. Budzelaar, K. Krogh-Jespersen, T. Clark, P. von R. Schleyer, *J. Am. Chem. Soc.* **1985**, *107*, 2113–2119.
- [26] J. Singha, Y. Wang, G. Raabe, *Z. Naturforsch. A* **2010**, *65*, 113–122.
- [27] G. E. Herberich, B. Hessner, *Chem. Ber.* **1982**, *115*, 3115–3127.
- [28] M.-A. Légaré, G. Bélanger-Chabot, G. De Robillard, A. Languérand, L. Maron, F.-G. Fontaine, *Organometallics* **2014**, *33*, 3596–3606.
- [29] J. A. K. Howard, I. W. Kerr, P. Woodward, *J. Chem. Soc. Dalton Trans.* **1975**, 2466–2469.
- [30] a) H. Fallah-Bagher-Shaidaei, C. S. Wannere, C. Corminboeuf, R. Puchta, P. von R. Schleyer, *Org. Lett.* **2006**, *8*, 863–866; b) Z. Chen, C. S. Wannere, C. Corminboeuf, R. Puchta, P. von R. Schleyer, *Chem. Rev.* **2005**, *105*, 3842–3888.
- [31] CCDC 1447233 (**1**), 1447234 (**2**) and 1447235 (**3**) contain the supplementary crystallographic data for this paper. These data can be obtained free of charge from Cambridge Crystallographic Data Centre.

Received: March 8, 2016

Revised: April 6, 2016

Published online: July 4, 2016